Solvent Effects on the $S_0(1^1A_g^-) \rightarrow S_2(1^1B_u^+)$ Transition of β-Carotene, Echinenone, Canthaxanthin, and Astaxanthin in Supercritical CO_2 and CF_3H

Zhenguo Chen, Changyoul Lee, Thomas Lenzer, and Kawon Oum*

Institut für Physikalische Chemie, Universität Göttingen, Tammannstrasse 6, D-37077 Göttingen, Germany

Received: July 10, 2006; In Final Form: August 10, 2006

Solvent-induced spectral shifts of the four C_{40} carotenoids, β-carotene, echinenone, canthaxantin, and astaxanthin, have been studied in supercritical CO_2 and CF_3H. In situ absorption spectroscopic analysis was used to determine the maximum peak position of the electronic transitions from the ground state ($1^1A_g^-$) to the S_2 state ($1^1B_u^+$) of the carotenoids. The medium polarizability function, $R(n) = (n^2 - 1)/(n^2 + 2)$ of the refractive index of the solvent was varied over the range $R(n) = 0.08-0.14$, by changing the pressure of CO_2 or CF_3H between 90 and 300 bar at the temperature 308 K. For all the carotenoids studied here, a significant hypsochromic shift of ca. 20−30 nm was observed in supercritical fluids as compared to that in nonpolar liquids. The spectral shifts in supercritical fluids were compared with those in liquids and showed a clear linear dependence on the medium polarizability. The temperature-dependent shift of the absorption maxima was less significant. Interestingly, there was almost no difference in the energetic position of the absorption maxima in supercritical CO_2 and CF_3H at a given $R(n)$ value. This is in contrast to previous extrapolations from studies in liquids at larger $R(n)$ values, which yielded different slopes of the $R(n)$-dependent spectral shifts for polar and nonpolar solvents toward the gas-phase limit of $R(n) = 0$. The current experimental results in the gas-to-liquid range show that the polarity of the solvent has only a minor influence on the $1^1A_g^- \rightarrow 1^1B_u^+$ transition energy in the region of low $R(n)$. We also obtain more reliable extrapolations of this 0−0 transition energy to the gas-phase limit $\nu_{0-0}^{\text{gas-phase}} \approx (23\,000 \pm 120)$ cm^{-1} for β-carotene.

1. Introduction

The roles of carotenoids as light-harvesting and photoprotective pigments are determined by the photochemistry of their low-lying excited electronic states.[1,2] A knowledge base of the energetics of these carotenoid excited electronic states and their dependence on conjugation length, the presence of substituents, isomeric structure, and solvent environment is a prerequisite for understanding the interactions of carotenoids involved in photobiology. Since direct gas-phase spectral measurements of carotenoids are extremely difficult to perform, one needs to estimate such energetics by extrapolating the transition energies in solvents to vacuum as outlined next.

The solvatochromic shifts of electronic absorption spectra in different solvents are the experimental evidence for the difference in solvation energies of the ground electronic state and the Franck−Condon excited electronic state. The solvatochromic shifts are generally related to dielectric interactions between solute and solvent molecules when they depend only on multipole and polarizability properties of the solute and solvent molecules.[3] In addition, specific interactions such as hydrogen bonding can influence the spectral shape and the shift of the peak positions.[3]

Especially, solvent-induced absorption spectral shifts of the electronic transition from the ground ($1^1A_g^-$) state to the second-excited state ($1^1B_u^+$) of carotenoids have been intensively studied in liquids. Andersson et al. have measured the spectral shifts of the absorption for β-carotene, lycopene, spheroidene, and spheroidenone in various nonpolar and polar solvents.[4] These measurements showed that the shift depends linearly on the solvent polarizability, and the energetic position of the absorption band maximum of β-carotene is well-correlated with the Lorentz−Lorenz function $R(n) = (n^2 - 1)/(n^2 + 2)$ of the refractive index of the solvent. This was attributed to a dispersive effect resulting from the high polarizability of the S_2 state.[4] Noguchi et al. also observed that absorption maxima of β-carotene, 8′-β-apo-8′-carotenal, and ethyl-8′-β-apo-8′-carotenoate are linearly correlated with $R(n)$ for each solvent.[5]

Interestingly, when the absorption maxima (in cm^{-1}) are plotted on the $R(n)$ scale, polar and nonpolar solvents showed different line slopes: the slope for polar solvents was flatter than that for nonpolar solvents over the range $R(n) = 0.2-0.4$, and both lines were crossing at the $R(n)$ value of about 0.3 (e.g., for spheroidene[6,7] and for neurosporene and β-carotene).[7] In the case of β-carotene, the maximum of the entire electronic absorption band of the $1^1B_u^+$ state in nonpolar solvents was expressed by Macpherson and Gillbro as:[8]

$$\tilde{\nu}(1^1B_u^+)^{\text{nonpolar}} = [25\,080 - 12\,060R(n)]\ \text{cm}^{-1}$$

while in polar solvents

$$\tilde{\nu}(1^1B_u^+)^{\text{polar}} = [23870 - 8181R(n)]\ \text{cm}^{-1} \qquad (2)$$

Nagae et al.[7] suggested similar expressions $\tilde{\nu}(1^1B_u^+)^{\text{nonpolar}} = [24\,976 - 12\,178R(n)]$ cm^{-1} for nonpolar solvents and $\tilde{\nu}(1^1B_u^+)^{\text{polar}} = [23\,787 - 8268R(n)]$ cm^{-1} for polar solvents. They developed a theory to explain this observation such that, in polar solvents, an electric field that is generated by fluctuation of the solvent dipoles affects the conjugated chain of the carotenoid in a long spheroidal cavity; it stabilizes the $1^1B_u^+$ energy through

* Corresponding author. E-mail: koum@gwdg.de; tel: +49 551 3912598, fax: +49 551 393150.

10.1021/jp0643247 CCC: $33.50
Published on Web 09/14/2006

the polarization effect (leading to a larger stabilization relative to nonpolar solvents when extrapolating $R(n)$ to 0) and substantially reduces the dispersive interaction (resulting in a smaller slope). Renge et al. also assigned different linear regression parameters for the dependence of absorption maxima of β-carotene in nonpolar *n*-alkanes, $\tilde{\nu}(^1B_u^+)^{nonpolar} = [24\,260 - 8994R(n)]\ cm^{-1}$, while in polar solvents, $\tilde{\nu}(^1B_u^+)^{polar} = [22\,298 - 428\{R(\epsilon) - R(n)\}]\ cm^{-1}$, where $R(\epsilon) = (\epsilon - 1)/(\epsilon + 2)$, and the difference between $\{R(\epsilon) - R(n)\}$ can be used as a measure of (di)polarity.[9]

Such different line slopes and consequently different intercepts at the limit $R(n) \rightarrow 0$ for nonpolar and polar solvents seem to fit well with experimental data in liquids over the $R(n)$ range of 0.2−0.4. However, these expressions can certainly not be extrapolated to low $R(n)$, as they should yield the same value in the limit of isolated gas-phase molecules ($R(n) = 0$).

In this respect, it is desirable to measure spectral shifts at small values of $R(n)$ for solvents of different polarity. Note that the solubility and vapor pressure of carotenoids are generally very low,[10,11] and it is a very difficult task to perform such an experiment in the dilute gas phase. In this study, we employed supercritical fluids, which allow us to access the range of low $R(n)$. Furthermore, supercritical fluids such as CO_2 or CF_3H have the clear advantage that the medium polarizability is varied just by the density change without alteration of the chemical identity of the solvent species, in contrast to studies using liquids, where parameters such as polarizability, polarity, hydrogen-bonding capability, or molecular size are varied at the same time. In our case, we can therefore avoid possible complications by minimizing effects of multiparameter influences.

In the following, we present the density and temperature dependence of the absorption spectra of β-carotene, echinenone, canthaxanthin, and astaxanthin in supercritical CO_2 and CF_3H over the pressure range of 90−300 bar at $T = 308$ K. In this density range, we can vary $R(n)$ between 0.08 and 0.14 for nonpolar supercritical CO_2 and for polar supercritical CF_3H. Next, we provide strong experimental evidence that the absorption maxima in the gas-to-liquid region are very similar for supercritical CO_2 and for supercritical CF_3H, and therefore, the extrapolation to $R(n) \rightarrow 0$ yields a single value for the gas-phase species.

2. Experimental Procedures

An optical high-pressure cell was used for the quasi-static absorption measurement of solid solutes in supercritical fluids. This cell can be used at pressures up to 500 bar and temperatures up to 100 °C. It consists of two separate optical compartments. Both beam paths have an identical length (80 mm) and are sealed with two sapphire end windows (diameter 10 mm, thickness 10 mm). One of the compartments contained only supercritical CO_2 or CF_3H and was used as a reference. The second compartment for the sample was connected to the mixing chamber via a particle filter (5 μm pore size). The total volume of the sample cell and the mixing chamber was 18 mL. Two heat cartridges were embedded in the high-pressure cell body, and the temperature was regulated by a controller (Eurotherm). A syringe-type high-pressure pump (ISCO, DX100) was used to keep the chosen constant pressure. Compressed CO_2 or CF_3H was preheated to the desired temperature and passed on to the high-pressure cell. Our portable high-pressure cell was small enough to be installed inside the sample chamber of the spectrometer (Varian CARY 5E). Absorption spectra were measured over the wavelength range of 200−800 nm with a spectral resolution of 0.1 nm. Each spectrum in the sample cell was corrected by the reference spectrum measured in the supercritical fluid only. (There was, however, no significant change in reference spectra of CO_2 and CF_3H at different pressures.)

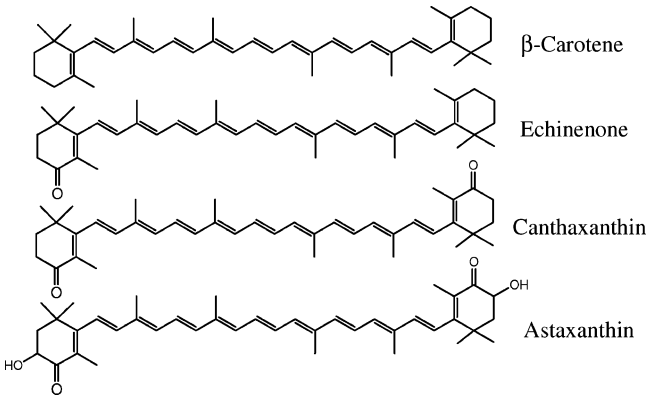

Figure 1. C_{40} carotenoids investigated in this paper.

Samples were prepared in the following way: first, we measured the solubility of carotenoids in supercritical fluids. For solubility measurements, about 1 mg of the carotenoid was loaded in the mixing cell and dissolved in supercritical fluids at a particular pressure and temperature with the help of a motor-driven magnetic stirrer. By doing this, only dissolved carotenoids were transferred into the sample cell through a particle filter. Absorption spectra were measured as a function of mixing time until they reached the solubility limit at a particular pressure and temperature of CO_2. Usually, this took about 1−3 h. For absorption measurements, we kept the carotenoid concentration far below the solubility limit. This required only a very small amount of the carotenoid (a few micrograms). Stock solutions of carotenoids were prepared in acetone (10^{-5} M), and the required amount (typically ca. 1×10^{-8} M) was pipetted directly into the mixing chamber. The liquid acetone was allowed to evaporate by heating the cell at 313 K. The sample cell and the mixing chamber were then pressurized at 90 bar, and sample stirring was initiated. By doing this, the loaded trace amount of carotenoids was completely dissolved in the supercritical fluid. Measurements were performed in the order of increasing pressure from 90 to 300 bar.

Carbon dioxide of 99.995 mass % purity (Praxair) and CF_3H of the same purity (Gerling Holz Co.) were used as received. Figure 1 contains structures for the C_{40} carotenoids studied in this paper. The highly purified β-carotene, echinenone, canthaxanthin, and astaxanthin were in all-trans (all-*E*) configurations with purity >97% and generously provided by BASF AG. The organic solvents had a purity ≥99%.

3. Results and Discussion

3.1. Solvent-Dependent Absorption Maxima of C_{40} Carotenoids. Figure 2 shows steady-state absorption spectra of β-carotene, echinenone, canthaxanthin, and astaxanthin in supercritical CO_2 ($p = 300$ bar, $T = 308$ K). The absorption band near 450 nm corresponds to the S_0 ($1^1A_g^-$) → S_2 ($1^1B_u^+$) transition. For comparison, we show their absorption spectra in *n*-hexane or in toluene. Interestingly, for all four carotenoids, a significant hypsochromic spectral shift was seen in supercritical fluids relative to the absorption maxima in *n*-hexane (∼20 nm) or toluene (∼30 nm). This is consistent with a preliminary investigation by Hui et al. of the behavior of the electronic absorption spectra of β-carotene, lycopene, zeaxanthin, canthaxanthin, and astaxanthin in supercritical CO_2.[12]

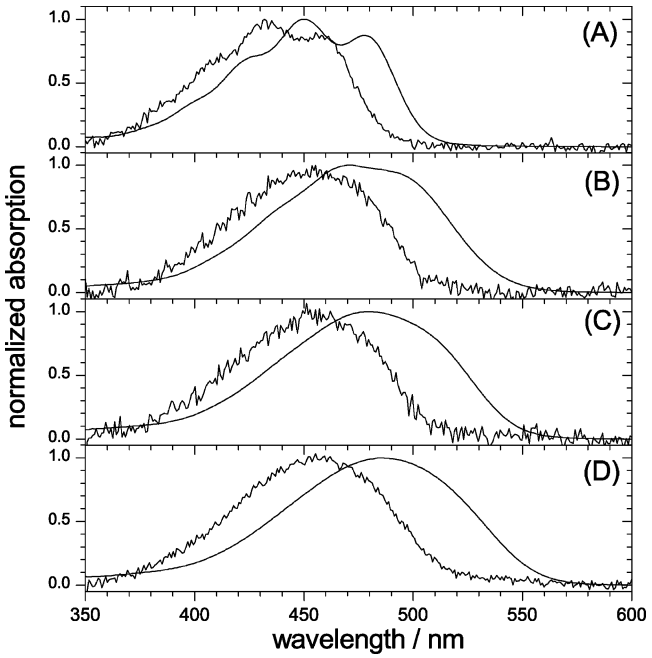

Figure 2. Steady-state absorption spectra of four different C_{40} carotenoids in supercritical CO_2 ($p = 300$ bar, $T = 308$ K, left solid line) and in room-temperature liquids (right solid line). Carotenoids are (A) β-carotene, (B) echinenone, (C) canthaxanthin, and (D) astaxanthin. For panel A, data in *n*-hexane are compared, while for panels B−D, data in toluene are shown for comparison.

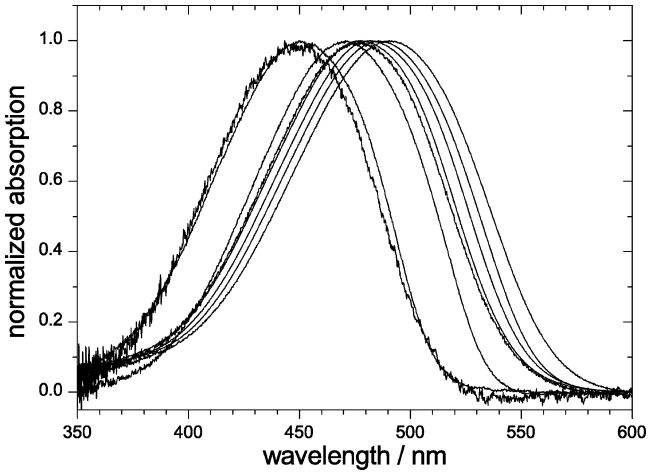

Figure 3. Steady-state absorption spectra of astaxanthin. From left to right: in supercritical CF_3H ($p = 200$ bar, $T = 308$ K) from this paper, in supercritical CO_2 ($p = 200$ bar, $T = 308$ K) from this paper, and in room-temperature liquids (*n*-hexane, methanol, acetone, tetrahydrofuran, toluene, and chloroform, respectively) from ref 13.

Absorption spectra of astaxanthin, for example, were structureless in the visible region both in supercritical CO_2 and in supercritical CF_3H. They were almost identical in terms of the position of the absorption maximum and the bandwidth (fwhm of ca. 100 nm). In Figure 3, we compare absorption spectra of astaxanthin in various room-temperature liquids (polar and nonpolar)[13] with those in supercritical CO_2 and CF_3H. Absorption maxima of the band near 450 nm are shifted to longer wavelengths in liquids as the solvent polarizability increases.

The effect of density change on the absorption maximum of astaxanthin in supercritical CO_2 is seen in Figure 4 over the pressure range of 100−300 bar at 308 K. Table 1 summarizes all experimental data mentioned in this paper. At higher

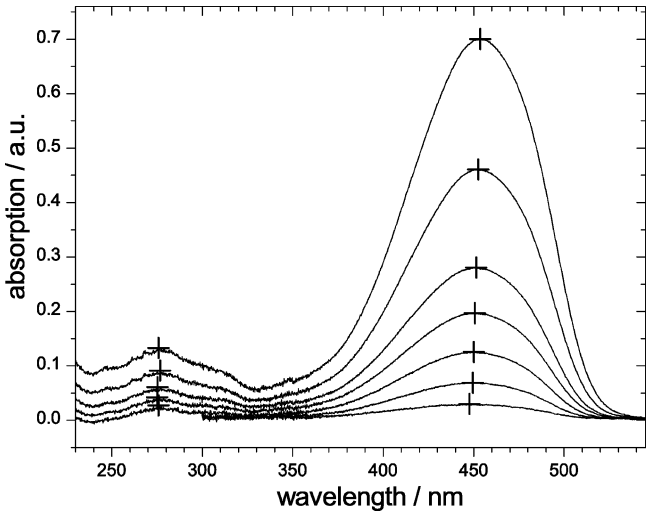

Figure 4. Absorption spectra of astaxanthin in supercritical CO_2 at 308 K at pressures of 100, 125, 150, 175, 200, 250, and 300 bar (from bottom to top). The crosses indicate the absorption maxima of the $1^1B_u^+$ (near 450 nm) and the $2^1B_u^+$ transitions (near 280 nm).

pressures, the position of the main peak of the S_0 ($1^1A_g^-$) → S_2 ($1^1B_u^+$) transition was shifted by ca. 6 nm to a longer wavelength (447.6−453.7 nm). In addition to the main absorption in the visible region, a weaker absorption band was observed between 250 and 300 nm, which is assigned to the $1^1A_g^- \rightarrow 2^1B_u^+$ transition.[1] Interestingly, the shift of this peak was insignificant, and the position of its absorption maximum was almost independent of pressure (see Figure 4). Obviously, the $1^1B_u^+$ and $2^1B_u^+$ transitions are affected to a different extent by the solvent polarizability, in a similar way as Hui et al.[12] and Kuki et al.[6] interpreted. We also mention that the so-called cis-peak, which is assigned to the $^1A_g^+$ transition and expected to appear near 350 nm,[14,15] was not observed in Figure 4, indicating that no complications with thermally- or photochemically-induced trans−cis isomerization occurred in our experiments.

The larger intensity of absorption signals at higher pressures in Figure 4 points to a better solubility of astaxanthin in supercritical CO_2. So far, there has been no report on the solubility of astaxanthin in supercritical fluids. Assuming that the absorption coefficients in supercritical CO_2 are the same as the values observed in liquids ($\epsilon_M \approx 10^5$ M^{-1} cm^{-1}), we could determine the solubility of astaxanthin to be in the range of 10^{-8} to 10^{-7} M under our experimental conditions. However, in several cases, it has been found that the experimentally recovered ϵ_M values in supercritical fluids were different from those in liquids and even they were density-dependent. This will be discussed in more detail next.

The absorption spectrum (in units of cm^{-1}) for β-carotene in 300 bar CO_2 at 308 K is shown in Figure 5. The vibronic structure of the spectrum is broadened presumably because nonplanarity between the central polyene chain and the terminal β-ionone rings results in a distribution of slightly differently absorbing species.[1] The absorption maxima of the 0−0 up to 0−4 transitions were analyzed by a sum of Gaussian peaks with a constant energetic width for the five individual peaks. An example for the analysis is shown in Figure 5. For instance, in 300 bar CO_2 at 308 K, the 0−0, 0−1, 0−2, 0−3, and 0−4 transitions occurred at 21 723, 23 152, 24 580, 26 009, and 27 438 cm^{-1}, respectively. As the pressure decreased to 90 bar, the five individual peaks of β-carotene shifted to higher energy, and the bandwidth decreased (e.g., from 1238 cm^{-1} at 300 bar to 1150 cm^{-1} at 90 bar). In the case of β-carotene, the absorption

TABLE 1: Absorption Maxima of β-Carotene and Astaxanthin in Various Solvents[a]

β-carotene in nonpolar solvents

solvent	$R(n)$	$R(\epsilon)$	ν_{max} (cm^{-1})	λ_{max} (nm)	ref	solvent	$R(n)$	$R(\epsilon)$	ν_{max} (cm^{-1})	λ_{max} (nm)	ref
n-hexane	0.229	0.228	22220	450.0	8	*n*-octane	0.241	0.240	22092	452.7	9
cyclohexane	0.255	0.255	21980	455.0	8	*n*-decane	0.248	0.248	22080	452.9	9
toluene	0.293	0.315	21570	463.6	8	*n*-undecane	0.255	0.249	21990	454.8	9
CS_2	0.357	0.352	20700	483.1	8	*n*-tetradecane	0.258	0.256	21925	456.1	9
n-pentane	0.219	0.220	22304	448.4	9	*n*-hexadecane	0.261	0.259	21906	456.5	9
n-hexane	0.229	0.228	22163	451.2	9	PVB	0.287	0.404	21625	462.4	9
n-heptane	0.236	0.236	22134	451.8	9	PSt	0.338	0.339	21330	468.8	9

β-carotene in polar solvents

solvent	$R(n)$	$R(\epsilon)$	ν_{max} (cm^{-1})	λ_{max} (nm)	ref	solvent	$R(n)$	$R(\epsilon)$	ν_{max} (cm^{-1})	λ_{max} (nm)	ref
acetone	0.220	0.867	22030	453.9	8	quinoline	0.354	0.731	21010	476.0	8
diethyl ether	0.217	0.526	22200	450.5	8	diethyl ether	0.217	0.526	22198	450.5	9
ethanol	0.221	0.890	22120	452.1	8	acetonitrile	0.212	0.921	22060	453.3	9
THF	0.246	0.688	21830	458.1	8	methyl acetate	0.220	0.653	22070	453.1	9
dichloromethane	0.255	0.726	21620	462.5	8	acetone	0.220	0.867	22032	453.9	9
benzonitrile	0.308	0.892	21320	469.0	8	aniline	0.336	0.669	21095	474.0	this paper
benzyl alcohol	0.314	0.784	21280	469.9	8						

β-carotene in supercritical fluids at 308 K

$p(CO_2)$ (bar)	$R(n)$	$R(\epsilon)$	ν_{max} (cm^{-1})	λ_{max} (nm)	ref	$p(CF_3H)$ (bar)	$R(n)$	$R(\epsilon)$	ν_{max} (cm^{-1})	λ_{max} (nm)	ref
90	0.099	0.115	23386	427.6	this paper	90	0.085	0.615	23546	424.7	this paper
100	0.106	0.124	23321	428.8	this paper	150	0.098	0.661	23419	427.0	this paper
150	0.121	0.141	23214	430.8	this paper	200	0.103	0.677	23359	428.1	this paper
200	0.128	0.150	23164	431.7	this paper						
250	0.133	0.156	23129	432.4	this paper						
300	0.137	0.161	23071	433.4	this paper						

astaxanthin in liquids

solvent	$R(n)$	$R(\epsilon)$	ν_{max} (cm^{-1})	λ_{max} (nm)	ref	solvent	$R(n)$	$R(\epsilon)$	ν_{max} (cm^{-1})	λ_{max} (nm)	ref
n-hexane	0.229	0.228	21240	470.8	this paper	ethanol	0.221	0.890	20877	479.0	13
toluene	0.293	0.315	20540	486.8	13	THF	0.246	0.688	20717	482.7	13
methanol	0.203	0.914	21000	476.2	13	chloroform	0.267	0.559	20321	492.1	13
acetonitrile	0.212	0.921	20972	476.8	13	DMSO	0.283	0.938	20273	493.3	13
acetone	0.220	0.867	20919	478.0	13						

astaxanthin in supercritical fluids at 308 K

$p(CO_2)$ (bar)	$R(n)$	$R(\epsilon)$	ν_{max} (cm^{-1})	λ_{max} (nm)	ref	$p(CF_3H)$ (bar)	$R(n)$	$R(\epsilon)$	ν_{max} (cm^{-1})	λ_{max} (nm)	ref
100	0.106	0.124	22341	447.6	this paper	160	0.100	0.667	22260	449.2	this paper
125	0.115	0.135	22245	449.5	this paper	180	0.102	0.674	22252	449.4	this paper
150	0.121	0.141	22221	450.0	this paper	200	0.104	0.679	22249	449.4	this paper
175	0.125	0.146	22194	450.6	this paper	225	0.106	0.685	22161	451.2	this paper
200	0.128	0.150	22154	451.4	this paper	250	0.108	0.690	22153	451.4	this paper
250	0.133	0.156	22094	452.6	this paper	275	0.110	0.694	22151	451.5	this paper
300	0.137	0.161	22041	453.7	this paper	300	0.111	0.697	22144	451.6	this paper

[a] $R(n) = (n^2 - 1)/(n^2 + 2)$ and $R(\epsilon) = (\epsilon - 1)/(\epsilon + 2)$, with the index of refraction n and dielectric constant ϵ of the solvent.

maximum of the band was almost identical to the fitted value of the 0−1 transition. We also measured pressure-dependent absorption spectra of β-carotene in supercritical CF_3H at 308 K. There were still noticeable vibronic features of the $1^1A_g^- \rightarrow 1^1B_u^+$ absorption band, and the absorption maxima were almost identical to those in supercritical CO_2 at the same $R(n)$ value. The $R(n)$ values for supercritical CO_2 and CF_3H were estimated from the work of Lewis et al.[16]

The pure thermochromic shift can be easily analyzed in supercritical fluids because the density can be kept constant when varying the temperature by adjusting the pressure. For example, the absorption maxima for β-carotene dissolved in supercritical CO_2 were found to be insensitive to the temperature change itself: when the pressure and temperature were varied at a constant density of $\rho = 0.93$ g/mL ($p = 300$, 338, 376, and 414 bar at temperatures of 308, 313, 318, and 323 K, respectively), the positions of the absorption maxima were almost constant at a value of (433.4 ± 0.4) nm. In *n*-hexane, the situation was slightly more complicated. Figure 6 shows the effect of the temperature change on the wavelength for the maximum absorption of β-carotene and astaxanthin in *n*-hexane. The peak position (in cm^{-1}) was shifted from 22 220 to 22 390 cm^{-1} for β-carotene and from 21 200 to 21 530 cm^{-1} for astaxanthin over the temperature range of 299−333 K. These changes are probably due to a combined effect of temperature and density variation. For instance, in the case of β-carotene in supercritical CO_2, the change of density at a constant temperature of 308 K from 0.66 to 0.93 g/mL (from 90 to 300 bar, see Table 1) resulted in a shift of −315 cm^{-1}. In the *n*-hexane case in Figure 6, the density changes only from 0.62 to 0.65 g/mL over the temperature range of 299−333 K, and still a spectral shift of −169 cm^{-1} is observed. Therefore, there appears to be an additional temperature effect for *n*-hexane. In any case, on an absolute scale, this effect is very small as compared to the solvatochromic shifts, which are of primary interest in this paper. As a fine detail, we note that the slopes for the two C_{40} carotenoids in Figure 6 are different, so the absolute size of the shift is also carotenoid-dependent.

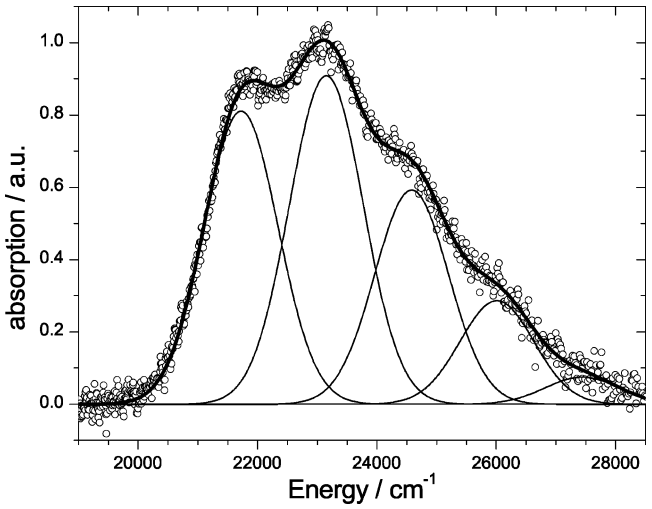

Figure 5. Steady-state absorption spectra of β-carotene in supercritical CO_2 ($p = 300$ bar, $T = 308$ K). Experimental data (open circles) are compared with a simulation result (thick line), which is the sum of five individual vibronic features of the transition (assumed to have a Gaussian shape). Simulation parameters: bandwidth = 1238 cm^{-1}, centers of transitions = 21 723 cm^{-1} (0−0), 23 152 cm^{-1} (0−1), 24 580 cm^{-1} (0−2), 26 009 cm^{-1} (0−3), and 27 438 cm^{-1} (0−4).

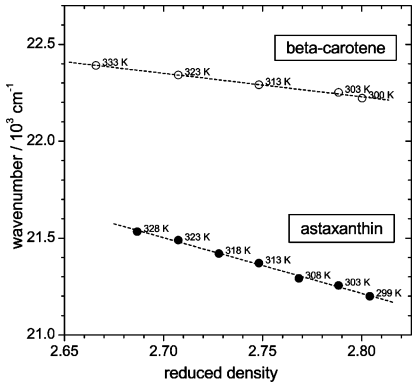

Figure 6. Temperature dependence of absorption maxima of β-carotene and astaxanthin in *n*-hexane over the temperature range of 299−333 K.

The spectral shifts of β-carotene and astaxanthin in various liquids as well as in supercritical CO_2 and CF_3H are summarized in Figures 7 and 8, respectively. These two figures are the main results of the current paper. Both figures show approximately linear relationships between the $1^1A_g^- \rightarrow 1^1B_u^+$ transition energy and the value of $R(n)$ for the set of nonpolar and polar solvents. In liquids, the absorption maxima for the polar solvents are on average located at lower energies than those for the nonpolar species. Deviations of some solvents from a strictly linear relationship are not surprising and show that a simple correlation with a single parameter like $R(n)$ will not be able to describe all details of spectral shift data. Interestingly, the difference in absorption maxima between polar and nonpolar solvents becomes less significant in supercritical CO_2 and CF_3H over the $R(n)$ range of 0.08−0.14: absorption maxima are very similar for β-carotene (Figure 7) and slightly smaller in the case of the polar CF_3H for astaxanthin (Figure 8). This is in contrast to previous extrapolation curves, which were solely based on the investigations in liquids. For comparison, we have also plotted the estimates of Macpherson and Gillbro[8] based on eqs 1 and 2 as dotted and dashed−dotted lines in Figure 7. Their extrapolations clearly deviate from the experimental data in

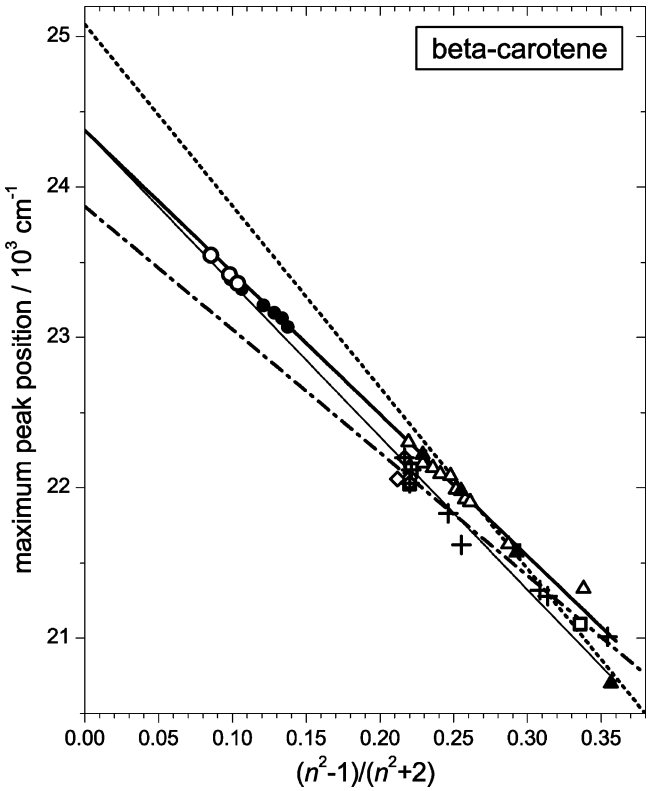

Figure 7. Solvatochromic shifts of the $S_0(1^1A_g^-) \rightarrow S_2(1^1B_u^+)$ transition of β-carotene in various solvents. Data of nonpolar liquids are from ref 8 (▲) and ref 9 (△). Data for polar liquids are from ref 8 (+) and ref 9 (◇). Additional data in aniline are from this paper (□). Supercritical fluid data in CO_2 (●) and in CF_3H (○) are from this paper. Lines are the results from linear regression: (thick solid line) from this paper for nonpolar solvents, (thin solid line) from this paper for polar solvents, (dotted line) from ref 8 for nonpolar solvents, and (dashed−dotted line) from ref 8 for polar solvents.

supercritical CO_2 and CF_3H. Including all data points of nonpolar and polar solvents together with our supercritical fluid data, we extrapolated to the $R(n) \rightarrow 0$ limit and obtained the following expressions for the absorption maxima of β-carotene in nonpolar solvents over the $R(n)$ range of 0−0.35:

$$\tilde{\nu}(^1B_u^+)^{\text{nonpolar}} = [(24\,376 \pm 120) - (9431 \pm 175)R(n)]\ \text{cm}^{-1} \quad (3)$$

while in polar solvents

$$\tilde{\nu}(^1B_u^+)^{\text{polar}} = [(24\,376 \pm 120) - (10\,178 \pm 178)R(n)]\ \text{cm}^{-1} \quad (4)$$

In a similar way, we summarize our results of absorption maxima of astaxanthin in Figure 8 with the following expressions over the $R(n)$ range of 0−0.30 in nonpolar solvents:

$$\tilde{\nu}(^1B_u^+)^{\text{nonpolar}} = [(23\,370 \pm 83) - (9549 \pm 170)R(n)]\ \text{cm}^{-1} \quad (5)$$

while in polar solvents

$$\tilde{\nu}(^1B_u^+)^{\text{polar}} = [(23\,370 \pm 83) - (11175 \pm 140)R(n)]\ \text{cm}^{-1} \quad (6)$$

The statistical error limits in eqs 3−6 correspond to 2σ standard deviations.

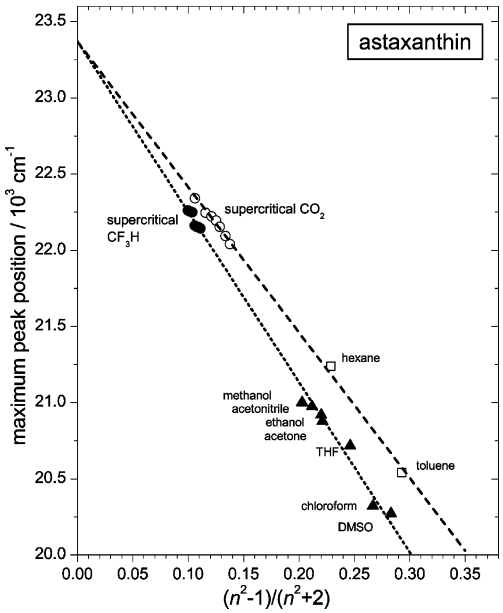

Figure 8. Solvatochromic shifts of the $S_0(1^1A_g^-) \rightarrow S_2(1^1B_u^+)$ transition of astaxanthin. Data for nonpolar (□) and polar (▲) liquids are from ref 13. Supercritical fluid data in CO_2 (○) and in CF_3H (●) are from this paper. Lines are the linear regression results from this work: (dashed line) for nonpolar solvents and (dotted line) for polar solvents.

We have further considered the influence of solvent polarity on the extrapolation of the location of absorption maxima, especially for some liquids with a dipolar character, following the method suggested by Renge et al.[9] with a bilinear function:

$$\tilde{\nu}(^1B_u^+) = [\tilde{\nu}_0 + aR(n) + b\{R(\epsilon) - R(n)\}]\ \mathrm{cm}^{-1} \quad (7)$$

where the *b* term is used to account for the effects of solvent (di)polarity.[9] All experimental data for *β*-carotene in both polar and nonpolar solvents in Table 1 are then expressed as

$$\tilde{\nu}(^1B_u^+) = [(24\,443 \pm 50) - (9796 \pm 190)R(n) - (318 \pm 50)\{R(\epsilon) - R(n)\}]\ \mathrm{cm}^{-1} \quad (8)$$

and for astaxanthin

$$\tilde{\nu}(^1B_u^+) = [(23\,546 \pm 50) - (10713 \pm 250)R(n) - (423 \pm 60)\{R(\epsilon) - R(n)\}]\ \mathrm{cm}^{-1} \quad (9)$$

with the linear regression coefficients 0.986 and 0.989, respectively. Much smaller values of the *b* terms as compared to the *a* terms in eqs 8 and 9 indicate that the spectral shifts are much more sensitive to the change of the solvent polarizability function $R(n)$. In any case, the resulting $\tilde{\nu}_0$ values in eqs 8 and 9 are in good agreement with the simpler extrapolation based on the polarizability of solvents in eqs 3−6.

For *β*-carotene, where the vibrational structure is well-resolved, we can further give an estimate for the 0−0 vibronic transition of the S_0 $(1^1A_g^-) \rightarrow S_2$ $(1^1B_u^+)$ band. Assuming that the difference between the 0−0 and the 0−1 peaks in the gas phase is similar to that in supercritical CO_2 at the lowest pressure measured in this study (ca. 1400 cm^{-1}), we can estimate that the 0−0 transition of *β*-carotene occurs at ca. (23 000 ± 120) cm^{-1} (∼435 nm). The use of eqs 3−9 yields a reasonable extrapolation to the limit $R(n) \rightarrow 0$ because of the collection of experimental data over a wide range of $R(n)$ values from the gas-to-liquid transition region into the liquid phase.

3.2. Density-Dependent Molar Absorption Coefficient ϵ_M of C_{40} Carotenoids. On-line ultraviolet/visible absorption spectroscopy is a standard procedure for the analysis of carotenoids by high-performance liquid chromatography. For such spectroscopic measurements of the solubility of solid samples, empirical calibration curves for the absorption-to-concentration conversion are required for a proper estimate of solubilities in supercritical fluids. Therefore, it is essential to obtain absorption spectra of C_{40} carotenoids in supercritical fluids and accurate information on solute molar absorption coefficients (ϵ_M). Furthermore, one has to consider that ϵ_M values of solutes in supercritical fluids are often temperature- and density-dependent. For example, Inomata et al. observed that IR absorption coefficients ϵ_M for naphthalene in supercritical CO_2 increased by a factor of 1.6 when changing the CO_2 density from 0.3 to 0.9 g cm^{-3}, by monitoring the intensity of an aromatic C−C vibrational mode at about 1600 cm^{-1}.[17] Frank and Roth observed an even more dramatic increase of the molar absorption coefficient associated with the O−D stretching mode of dilute HOD in water, which varied by nearly 2 orders of magnitude in the density range of 0.02−0.9 g cm^{-3}.[18] Specific mechanisms are, however, operative in such a hydrogen-bonded system. Closely related to our study, Rice et al., using electronic absorption spectroscopy, found that ϵ_M for anthracene and pyrene in supercritical CO_2 increased by a factor of 1.3−2.7 over the density range of 0.3−0.9 g cm^{-3}.[19] The origin of such density-dependent ϵ_M values observed in supercritical fluids from the IR to the UV−vis range is still not understood.

In this paper, we estimated the molar absorption coefficients of *β*-carotene, echinenone, canthaxanthin, and astaxanthin in supercritical CO_2 over the pressure range of 90−300 bar at 308 K in the following way: a known amount of C_{40} carotenoids was loaded in the high-pressure cell and dissolved in supercritical CO_2. The concentration was typically in the range of 1 × 10^{-8} M, which is at least 3−10 times lower than the solubility limit at the particular pressure at 308 K such that all carotenoids were completely dissolved already at the lowest pressure. This was confirmed by constant absorption signals of *β*-carotene as the CO_2 pressure was increased from 90 to 300 bar. However, surprisingly, the absorption signals of the other three carotenoids (astaxanthin, canthaxanthin, and echinenone) were consistently much weaker at lower CO_2 pressures than those expected in liquids for the same concentration. Since the number of carotenoid molecules should stay constant during the compression, the origin of such density-dependent absorption signal intensities is not clear. The decrease in absorption intensity at lower pressures was more visible in the order astaxanthin ≈ canthaxanthin > echinenone (see Figure 9). The experimental uncertainty (less than 10%) is too small to explain the difference in absorption intensities between 90 and 300 bar data. In Figure 9, we summarize the experimental observations for the four different C_{40} carotenoids and indicate apparent molar absorption coefficients at different densities in supercritical CO_2, in comparison with those measured in liquids. At this point, it is only possible to speculate on the reason for the observed effect. Aggregation of carotenoids at low densities could take place; however, it is likely to be accompanied by changes of the spectral shape (e.g., the appearance of additional bands to the red or blue of the monomer spectrum, which arise from exciton interactions). However, we observed that within our signal-to-noise ratio, the band shape was independent of concentration. It could also be that the observed changes are due to a pressure-dependent equilibrium between carotenoid molecules in solution and molecules adsorbed on the metal walls of the high-pressure

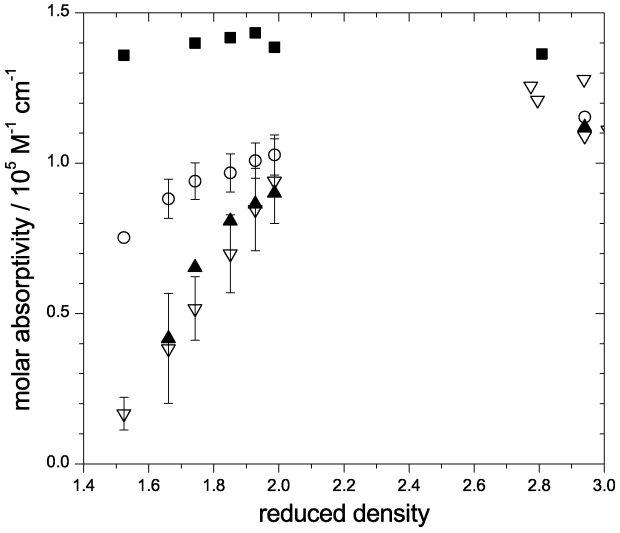

Figure 9. Density dependence of the apparent molar absorption coefficient in supercritical CO_2 over the pressure range of 90−300 bar at 308 K for (■) β-carotene, (○) echinenone, (▲) canthaxanthin, and (▽) astaxanthin. Values for liquids are from this paper in methanol ($\rho_r = 2.77$), tetrahydrofuran ($\rho_r = 2.80$), *n*-hexane ($\rho_r = 2.81$), acetone ($\rho_r = 2.94$), and toluene ($\rho_r = 2.94$).

cell. Finally, it is interesting to note that this unusual effect of the density-dependent absorption coefficient becomes weaker when the number of OH and C═O substituents is reduced. Further experimental studies are currently underway in our group to study this effect in more detail.

4. Conclusion

We have investigated solvent-induced spectral shifts of the C_{40} carotenoids β-carotene, echinenone, canthaxanthin, and astaxanthin in supercritical CO_2 and CF_3H. Our experimental data in the $R(n)$ range of 0.08−0.14 provide a clear way to extrapolate spectral shift data to the gas-phase limit such that one can more reliably estimate the 0−0 transition of the $1^1A_g^- \rightarrow 1^1B_u^+$ transition energy of carotenoids. In addition, we have reported apparent density-dependent molar absorption coefficients for echinenone, canthaxanthin, and astaxanthin in supercritical CO_2. The origin of such a variation is not yet clear.

Acknowledgment. Financial support from the Alexander von Humboldt foundation in the framework of the Sofja Kovalevskaja program and the German Science Foundation and helpful discussions with J. Troe, K. Luther, J. Schroeder, S. Beuermann, M. Buback, and J. Gierschner as well as very generous experimental support from R. Bürsing are gratefully acknowledged. We also thank the BASF AG, and especially Dr. Hansgeorg Ernst, for providing the highly purified carotenoid samples and extensive advice. Finally, we thank the referees for their helpful comments.

References and Notes

(1) Frank, H. A.; Young, A. J.; Britton, G.; Cogdell, R. J. *The Photochemistry of Carotenoids*, 1st ed.; Kluwer: Dordrecht, The Netherlands, 1999; Vol. 8.
(2) Polívka, T.; Sundström, V. *Chem. Rev.* **2004**, *104*, 2021.
(3) Suppan, P. *J. Photochem. Photobiol., A* **1990**, *50*, 293.
(4) Andersson, P. O.; Gillbro, T.; Ferguson, L.; Cogdell, R. J. *Photochem. Photobiol.* **1991**, *54*, 353.
(5) Noguchi, T.; Hayashi, H.; Tasumi, M.; Atkinson, G. H. *J. Phys. Chem.* **1991**, *95*, 3167.
(6) Kuki, M.; Nagae, H.; Cogdell, R. J.; Shimada, K.; Koyama, Y. *Photochem. Photobiol.* **1994**, *59*, 116.
(7) Nagae, H.; Kuki, M.; Cogdell, R. J.; Koyama, Y. *J. Chem. Phys.* **1994**, *101*, 6750.
(8) Macpherson, A. N.; Gillbro, T. *J. Phys. Chem. A* **1998**, *102*, 5049.
(9) Renge, I.; van Grondelle, R.; Dekker, J. P. *J. Photochem. Photobiol., A* **1996**, *96*, 109.
(10) Johannsen, M.; Brunner, G. *J. Chem. Eng. Data* **1997**, *42*, 106.
(11) Kraska, T.; Leonhard, K. O.; Tuma, D.; Schneider, G. M. *J. Supercrit. Fluids* **2002**, *23*, 209.
(12) Hui, B.; Young, A. J.; Booth, L. A.; Britton, G.; Evershed, R. P.; Bilton, R. F. *Chromatographia* **1994**, *39*, 549.
(13) Kopczynski, M.; Lenzer, T.; Oum, K.; Seehusen, J.; Seidel, M. T.; Ushakov, V. G. *Phys. Chem. Chem. Phys.* **2005**, *7*, 2793.
(14) Kuki, M.; Koyama, Y.; Nagae, H. *J. Phys. Chem.* **1991**, *95*, 7171.
(15) Fujii, R.; Furuichi, K.; Zhang, J.; Nagae, H.; Hashimoto, H.; Koyama, Y. *J. Phys. Chem. A* **2002**, *106*, 2410.
(16) Lewis, J. E.; Biswas, R.; Robinson, A. G.; Maroncelli, M. *J. Phys. Chem. A* **2001**, *105*, 3306.
(17) Inomata, H.; Yagi, Y.; Saito, M.; Saito, S. *J. Supercrit. Fluids* **1993**, *6*, 237.
(18) Franck, E. U.; Roth, K. *Discuss. Faraday Soc.* **1967**, *43*, 108.
(19) Rice, J. K.; Niemeyer, E. D.; Bright, F. V. *Anal. Chem.* **1995**, *67*, 4354.